

# LINC01956 promotes metastasis and M2 polarization of tumor-associated macrophages in glioblastoma via the FUS/ $\beta$ -catenin signaling pathway

**Gong Zhang**

Shanxi Medical University

**Fa Jin**

Southern Medical University

**Fengfei Lu**

Southern Medical University

**Lihong Zhao**

Shanxi Medical University

**xubin deng** (✉ [xubindeng@126.com](mailto:xubindeng@126.com))

Guangzhou Medical University Affiliated Cancer Hospital <https://orcid.org/0000-0003-0892-7284>

---

## Research Article

**Keywords:** LINC01956, FUS, GBM, tumor-associated macrophage, WNT/ $\beta$ -catenin signaling

**Posted Date:** June 1st, 2022

**DOI:** <https://doi.org/10.21203/rs.3.rs-1649253/v1>

**License:** © ⓘ This work is licensed under a Creative Commons Attribution 4.0 International License. [Read Full License](#)

---

# Abstract

Long noncoding RNAs (lncRNAs) can drive cancer progression. Here, we studied the role of a novel lncRNA, LINC01956, in glioblastoma (GBM). The level of LINC01956 was elevated in GBM cell lines and tissues. LINC01956 downregulation suppressed the migration and proliferation of GBM cells both in vitro and in vivo. Silencing of LINC01956 also significantly suppressed the growth of patient-derived organoids. M2 polarization of macrophages induced by exosomes derived from glioma cells overexpressing LINC01956 further accelerated GBM progression. Mechanistically, we found that FUS interacted with both LINC01956 and  $\beta$ -catenin. LINC01956 bound to FUS and reduced its ubiquitination. LINC01956 evoked nuclear translocation of phosphorylated (p)- $\beta$ -catenin by recruiting FUS. Furthermore, under hypoxic conditions, LINC01956 was regulated by HIF-1 $\alpha$ . Taken together, our data revealed for the first time that LINC01956 exerts pro-tumor effects via FUS-dependent activation of the WNT/ $\beta$ -catenin signaling pathway.

## Introduction

High-grade glioma, also called glioblastoma (GBM), is a kind of brain cancer characterized by diffuse invasion and resistance to treatment[1]. Currently, a combination of neurosurgery, radiotherapy and chemotherapy is a common treatment for GBM patients. However, glioblastoma patients usually have a poor prognosis, with a 5-year survival rate of less than 5%[2]. Hence, determining the mechanisms that underlie the progression of glioblastoma and searching for new therapeutic drugs is imperative.

Long noncoding RNAs (lncRNAs), defined as noncoding transcripts > 200 nucleotides in length, are involved in diverse biological processes[3]. Recent documents have demonstrated that dysregulation of lncRNAs is closely related to a variety of pathological conditions, including glioma[4].

Tumor-associated macrophages (TAMs) infiltrate most solid tumors, which leads to cancer progression[5]. TAMs are a subtype of pro-tumoral macrophages with transcriptional and phenotypic characteristics distinct from those of M1 and M2 macrophages[6]. Depending on the polarization state, macrophages can be converted into two main types, M1 and M2[7]. Recently, it was reported that lncRNAs can affect the polarization of TAMs[8].

Our previous studies have demonstrated that Wnt/ $\beta$ -catenin signaling is involved in the initiation and progression of various cancers[9, 10]. Wnt ligands secreted by glioma cells can activate Wnt/ $\beta$ -catenin signaling in macrophages and thereby induce M2 macrophage polarization[11].

In the present study, we identified LINC01956 as an onco-lncRNA in glioma. We explored the underlying mechanism of LINC01956 in glioma cell invasion and M2 macrophage polarization.

## Materials And Methods

### Cell culture and sample collection

GBM cell lines were purchased from the Chinese Academy of Science (Shanghai, China). Cells were maintained in DMEM supplemented with 10% fetal bovine serum (FBS) in a 37°C, 5% CO<sub>2</sub> incubator.

GBM and normal brain tissue samples were obtained from patients at People's Hospital of Shanxi Province and Zhujiang Hospital. Written informed consent was obtained from all patients prior to the study. All experiments

were performed in accordance with the approved guidelines of the Institutional Research Ethics Committee of Shanxi Medical University and Southern Medical University.

### **Culture of organoids**

The fresh glioma tissues were collected and cultured in advanced Dulbecco's modified Eagle's medium (DMEM)/F12, which contained 1% penicillin streptomycin. Subsequently, the glioma tissues were diced into approximately 2–3-mm sections, followed by digested at 37°C for 1 hour by trypsin. Then the digested tissues were filtered via 70 µm filter and the suspension was centrifuged. The cell pellet was resuspended in Matrigel, followed by plated in pre-warmed (37 °C) 24-well culture plates. The growth rate of organoids was monitored on the indicated times.

### **RT-PCR analysis**

To carry out RT-PCR analysis, total RNA was isolated from GBM cells by using TRIzol reagent (Invitrogen). Subsequently, this RNA was transcribed into cDNA by using HiScript II Q-RT SuperMix.

### **MTT assay**

First, GBM cells were seeded in 96-well plates and allowed to grow for 36 hours. Subsequently, the medium was aspirated, and MTT solution was added to each well. After 30 minutes, 150 µL of DMSO was added to each well, and the absorbance was read at an OD of 590 nm.

### **Colony formation assay**

GBM cells were seeded into 6-well culture plates and allowed to grow for two weeks. Subsequently, these cells were washed with phosphate-buffered saline (PBS) and stained with Giemsa solution.

### **Western blot analysis**

To extract protein, RIPA buffer was used to lyse GBM cells. Then, proteins were separated by SDS-PAGE and transferred to polyvinylidene fluoride (PVDF) membranes. Subsequently, membranes were blocked with 5% nonfat milk and incubated first with primary antibodies at 4°C overnight and then with HRP-conjugated secondary antibodies at room temperature for 1 hour. The levels of all proteins were determined by using enhanced chemiluminescence reagents.

### **Chromatin immunoprecipitation (CHIP) assay**

The ChIP assay was performed with a ChIP assay kit (Millipore, catalog: 17-371) as previously described[12]. Enrichment of DNA fragments at the putative HIF1-binding sites in the LINC01956 promoter was assessed by RT-PCR.

### **RNA-binding protein pulldown assay**

The RNA-binding protein pulldown assay was performed with a Pierce™ Magnetic RNA-Protein Pull-Down Kit (Thermo Fisher Scientific, MA, USA). The probe targeting LINC01956 was obtained from RiboBio, Guangzhou,

China. Protein was eluted from the beads and separated with SDS-PAGE. Subsequently, the protein bands on the gel were subjected to silver staining. Western blot analysis was used to identify the proteins.

### **RNA immunoprecipitation (RIP) assay**

The RIP assay was performed with a Magna RIP™ RNA-Binding Protein Immunoprecipitation kit (Millipore, Billerica, MA). The primary antibody against FUS was purchased from Santa Cruz (CA, USA). RT-PCR analysis was used to identify coprecipitated RNAs.

### **Immunofluorescence (IF) staining**

To carry out the IF assay, cells grown on sterile glass cover slips were fixed with 4% paraformaldehyde and permeabilized with Triton X-100. Cells were incubated first with primary antibodies and then with secondary antibodies. DAPI was used to counter stain nuclei. A Nikon eclipse Ti-E inverted fluorescence microscope was used to acquire images.

### **Biolayer interferometry (BLI)**

An Octet system (ForteBio, Fremont, CA) was used to carry out BLI. Biotin-labeled LINC01956 was immobilized on a streptavidin sensor.

### **Coimmunoprecipitation (co-IP) assay**

The interactions among LINC01956, FUS and  $\beta$ -catenin were validated by a co-IP assay that was described in a previous report[13].

### **Exosome isolation**

To isolate exosomes, culture medium from glioma cells was centrifuged first at 500×g for 5min and then at 2000×g for 30 min. Subsequently, 2×PEG solution was mixed with the supernatant. Later, the mixture was centrifuged at 10,000×g for 1 hour.

### **In vivo tumor growth experiment**

The care of animals was carried out in accordance with the approved guidelines of the Institutional Research Ethics Committee of Shanxi Medical University and Southern Medical University. Luciferase-expressing sh-LINC01956 cells and sh-ctrl cells were injected into the brain parenchyma of nude mice using a previously described protocol[14]. Glioma xenografts were monitored at 7 and 21 days after cell injection via an IVIS Spectrum Live Imaging System (Caliper Life Sciences, Mountain View, CA).

## **Results**

### **The expression level of LINC01956 is elevated in GBM tissues and associated with poor clinical outcome**

The Cancer Genome Atlas (TCGA) database was used to investigate the expression of lncRNAs in glioma and normal brain tissues (fold change>2, Supplementary Figure 1A). We examined the expression levels of the top thirty lncRNAs that were significantly increased in glioma tissues (Supplementary Figure 1 B) by RT-PCR. We

found that the expression level of LINC01956 was elevated in glioma tissues compared with normal brain tissues (Figure 1A); therefore, we selected LINC01956 for further study. This finding was also confirmed by using the GEPIA server (<http://gepia.cancer-pku.cn/>, which analyzes data from TCGA and GTEx, Figure1B). In addition, GBM patients with a high expression level of LINC01956 tended to have poorer overall survival and disease-free survival rates than those with low expression levels of LINC01956(Figure1C and D, data analyzed with GEPIA). The time ROC analysis was carried out to compare the predictive accuracy and risk score of LINC01956 for OS and DFS in glioma by using the TCGA database. In the OS analysis, LINC01956 expression level could predict the prognosis of glioma patients at 1, 3 and 5 years, and its AUC under the ROC curve was 0.75, 0.808 and 0.725, respectively(Supplementary Figure 1C). In the DFS analysis, AUC under the ROC curve was 0.75, 0.805 and 0.734, respectively(Supplementary Figure 1D). These data fully implicated that LINC01956 could be an ideal marker for predication of OS and DFS in glioma.

### **Correlation of LINC01956 expression levels with clinicopathological features in glioma**

We then analyzed the correlation of LINC01956 expression levels with clinicopathological features in glioma by mining the data from TCGA. It was found that LINC01956 expression levels increased gradually with the glioma WHO grades. Glioma patients with WHO grade 4 had the highest expression level of LINC01956 than other patients(Supplementary Figure 1E). In addition, LINC01956 expression level was highly expressed in glioblastoma patients, when compared with that in other histological types(Supplementary Figure 1F). We also found that LINC01956 expression level was decreased in IDH mutant patients when compared with that in IDH wild type patients(Supplementary Figure 1G). Interestingly, LINC01956 expression level was significantly associated with patient treatment outcome. In glioma patients with poor outcome(progressive disease), the LINC01956 expression level was significantly higher than that in those patients with clinical benefit (complete response, partial response and stable disease) (Supplementary Figure 1H). In the univariate analysis, WHO grade, 1p/19q codeletion, IDH status, histological type and LINC01956 expression level affected the prognosis of glioma patients (all  $p < 0.05$ ).Furthermore, multivariate cox regression showed that the above characteristics were also independent risk factors for unfavorable OS of glioma(Table 1).

### **LINC01956 inhibition decreases GBM cell growth and invasion**

Firstly, genes coexpressed with LINC01956 ( $|\log FC| \geq 1$ ,  $P_{adj} < 0.05$ ) were selected to perform gene enrichment analysis, followed by GO term analysis. The biological process (BP) analysis showed positive regulation of cell cycle process, positive regulation of cell cycle phase transition, epithelial cell proliferation and positive regulation of cell-cell adhesion. The cellular component (CC) analysis showed that spindle, spindle microtubule and collagen-containing extracellular matrix were significantly enriched. The molecular function (MF) analysis showed that growth factor activity, chemokine activity, cytokine receptor binding and cytokine activity were significantly enriched. In the KEGG analysis, we found that cell cycle, cell adhesion molecules and focal adhesion were significantly enriched(Supplementary Figure 1I). These data implicated that LINC01956 may participate in cell signaling functions that regulate proliferation and invasion of glioma.

Based on the above findings, we then performed biological function assay to analyze LINC01956's function on glioma cell proliferation and invasion. GBM cell lines (U87 and U251) were used in this functional study. First, we established cells in which LINC01956 was stably knocked down (sh-LINC01956) and a control cell group, namely, sh-ctrl (Figure 2A). Cell growth was examined by MTT and colony formation assays. As revealed by the MTT

assay, LINC01956 downregulation decreased cell viability (Figure 2B). In parallel, the colony formation assay revealed that sh-LINC01956 cells formed smaller and fewer colonies than sh-ctrl cells (Figure 2C, Supplementary Figure 1J). We further sought to determine whether LINC01956 affects the cell cycle distribution. The frequency of GBM cells in G1 phase was significantly higher than that in S phase when LINC01956 was knocked down, as revealed by flow cytometric analysis (Figure 2D, Supplementary Figure 1K). In parallel, G1/S cell cycle checkpoint proteins (e.g., cyclinD1 and CDK4) were downregulated in sh-LINC01956 cells (Figure 2E). Together, these findings imply that LINC01956 promotes the transition from G1 to S phase and thus promotes GBM cell growth in vitro. The Boyden chamber assay showed that LINC01956 inhibition decreased the invasion ability of GBM cells (Figure 2F, Supplementary Figure 1L). Subsequently, we analyzed the expression levels of epithelial-mesenchymal transition (EMT)-related proteins by western blot analysis. Interestingly, LINC01956 downregulation inhibited N-cadherin and vimentin expression and elevated E-cadherin expression levels (Figure 2G). These data suggested that downregulation of LINC01956 reversed the EMT phenotype.

Subsequently, we sought to determine whether LINC01956 has an effect on cell growth in vivo. To this end, luciferase-expressing U87 cells transduced with sh-ctrl or sh-LINC01956 were injected into the brains of nude mice to establish an orthotopic glioma xenograft model. We observed that the growth of sh-LINC01956-transduced cells was significantly slower than that of sh-ctrl-transduced cells (Figure 2H). These findings indicate that downregulation of LINC01956 inhibits tumorigenesis of glioma cells in vivo.

### **LINC01956 is a potential target in patient-derived glioma organoid model**

We established personalized patient-derived organoid (PDO) models to further investigate whether LINC01956 could be a potential target for glioma. As revealed in Figure 2I, down-regulation of LINC01956 significantly suppressed the glioma cell growth in two PDO models. Thus, our data suggest that LINC01956 could be a potential target in glioma patients.

### **LINC01956 promotes GBM cell progression via the WNT/ $\beta$ -catenin signaling pathway**

We next performed RNA sequencing to examine the difference in transcript expression levels between sh-ctrl and sh-LINC01956 cells (fold change > 2). Gene ontology analysis, KEGG pathway enrichment and Gene Set Enrichment Analysis (GSEA) analysis revealed that the WNT/ $\beta$ -catenin pathway was significantly altered when LINC01956 was downregulated (Supplementary Figure 2A-D). Western blot analysis revealed that downregulation of LINC01956 decreased the levels of phosphorylated  $\beta$ -catenin and its downstream targets (c-myc and cyclinD1, Figure 3A). The immunofluorescence assay revealed that downregulation of LINC01956 impaired the translocation of  $\beta$ -catenin into the nucleus (Figure 3B). In addition, downregulation of LINC01956 markedly decreased TOP/FOP transcriptional activity (Figure 3C). These data suggest that downregulation of LINC01956 suppresses WNT/ $\beta$ -catenin signaling pathway activity.

To examine whether the WNT/ $\beta$ -catenin pathway mediates the effect of LINC01956 on GBM cell progression, we used LiCl (a key activator of the WNT/ $\beta$ -catenin pathway) to perform rescue experiments in LINC01956-silenced cells. As expected, the suppressive effect of LINC01956 downregulation on cell viability and proliferation was significantly reduced in the context of LiCl addition (Figure 3D-E). In parallel, both the cell invasion ability and cell cycle distribution, which were affected by LINC01956 downregulation, were restored after WNT/ $\beta$ -catenin pathway activation (Figure 3F-G). Collectively, our data suggest that the WNT/ $\beta$ -catenin pathway mediates the pro-motive effect of LINC01956 on GBM development.

## **LINC01956 binds to FUS and reduces its ubiquitination**

RT-PCR showed that LINC01956 is localized in both the cytoplasm and the nucleus (Supplementary Figure 3A). The starBase database (<http://starbase.sysu.edu.cn/starbase2/rbpLncRNA.php>) was used to identify interactions between LINC01956 and potential RNA-binding proteins (RBPs). Among these RBPs, we found that there were three RBPs (FUS, NOP56 and TIA1) that interacted with LINC01956 (Supplementary Figure 3B). We focused on FUS because FUS participated in the regulation of GBM cell progression. We performed a series of experiments to confirm the association between LINC01956 and FUS. We used SDS-PAGE to isolate proteins complexes pulled down with a probe targeting LINC01956. Among the bands, that the band corresponding to FUS was present in the immune blot of the precipitate pulled down with the probe targeting LINC01956 and not in that pulled down with the control probe (Supplementary Figure 3C). RNA pull-down and RIP assays revealed that LINC01956 directly interacted with FUS in U87 and U251 cells (Figure 4A). Furthermore, we used a series of LINC01956 deletion mutants to map the FUS binding region. We found that LINC01956 mutant  $\Delta 3$  bound to FUS as efficiently as full-length LINC01956, whereas the binding capacity of the other mutants was completely abolished (Figure 4B). Via an immunofluorescence assay, we identified colocalization of LINC01956 and FUS in GBM cells (Figure 4C). We then demonstrated that the total protein level of FUS was decreased by LINC01956 inhibition, while its mRNA level was not altered (Figure 4D). Subsequently, a cycloheximide (CHX) chase assay was performed to examine whether LINC01956 can maintain FUS protein stability. The half-life of the FUS protein was significantly decreased to approximately 16 hours in cells with LINC01956 downregulation, whereas it was greater than 24 hours in the control group, as revealed by western blot analysis (Figure 4E). The ubiquitination assay revealed a significant increase in polyubiquitinated FUS protein in cells with LINC01956 downregulation (Figure 4F).

Taken together, these data suggest that LINC01956 binds to FUS and reduces its ubiquitination.

## **LINC01956 facilitates the translocation of $\beta$ -catenin into the nucleus of GBM cells by recruiting FUS**

The interaction between FUS and  $\beta$ -catenin was predicted by starBase (Supplementary Figure 3B). The co-IP assay was performed to confirm the interaction between FUS and  $\beta$ -catenin (Figure 5A). We then sought to determine whether FUS mediates LINC01956's effect on the WNT/ $\beta$ -catenin signaling pathway. The two-step co-IP assay revealed that tagged  $\beta$ -catenin and FUS were both present in the anti-hemagglutinin (HA)-precipitated complex enriched with LINC01956. Similarly, HA- $\beta$ -catenin and FLAG-FUS coprecipitated with LINC01956-FLAG but not with immunoglobulin G (IgG) (Figure 5B). These data suggest that  $\beta$ -catenin, FUS and LINC01956 form a complex. In addition, we observed that overexpression of FUS counteracted the decrease in the level of nuclear phosphorylated (p) $\beta$ -catenin in sh-LINC01956 GBM cells (Figure 5C). In parallel, the immunofluorescence assay revealed that downregulation of LINC01956 inhibited nuclear translocation of  $\beta$ -catenin and that this effect was abrogated in the context of FUS cotransfection (Figure 5D). Taken together, we speculate that LINC01956 leads to nuclear translocation of activated  $\beta$ -catenin in cooperation with FUS.

## **Exosomal LINC01956 promotes M2 polarization of macrophages**

The tumor-infiltrating lymphocytes may affect prognosis of various of cancer, including glioma. We then explored the association between LINC01956 and 24 immune-cell subsets in glioma by means of ssGSEA with Spearman  $r$ . The data were present in supplementary Figure 2D. Among the analysis, the significant correlation between LINC01956 and infiltration levels of macrophages caught our attention. Because activation of the Wnt/

$\beta$ -catenin pathway contributes to M2 polarization; we thus sought to determine whether LINC01956 affects M2 polarization. To this end, we evaluated the expression levels of LINC01956, M1 markers, and M2 markers in unpolarized macrophages, LPS/INF- $\gamma$ -induced M1 macrophages, and IL-4/IL-13-induced M2 macrophages. We observed elevated expression of M1-associated genes (CD80, MCP-1 and iNOS) in M1 macrophages and of M2-associated genes (CD206 and MRC-2) in M2 macrophages (Figure 6A). This result indicates the successful polarization of macrophages. Compared with that in M1 macrophages, the expression level of LINC01956 in M2 macrophages was elevated (Figure 6B). These data suggest that LINC01956 is involved in macrophage polarization. Subsequently, we treated THP-1 cells with PMA for 24 hours, transfected them with si-ctrl or si-LINC01956 and added IL-4 and IL-13 to induce polarization toward the M2 phenotype. In si-LINC01956 cells, the levels of M1 markers were markedly increased, and the levels of M2 markers were significantly decreased (Figure 6C). In contrast, LINC01956 overexpression led to the opposite result (Figure 6D). In addition, when compared with supernatant from control cells, supernatant from pcDNA-LINC01956 cells led to increased expression of M2 markers (Figure 6E).

Subsequently, we explored the interactions between GBM cells and macrophages. Previous studies demonstrated that lncRNAs can be transferred by exosomes and thereby regulate the tumor microenvironment (TME) [15]. We hypothesized that LINC01956 may be transferred in this way. We isolated exosomes from the supernatants of cultured GBM cells and measured the levels of the exosome-related proteins CD63, HSP70, and HSP90 by western blot analysis (Figure 6F). Downregulation of LINC01956 led to decreased levels of LINC01956 in the secreted exosomes (Figure 6G). These data proved the existence of LINC01956 in exosomes. Subsequently, we cocultured unpolarized macrophages with exosomes isolated from pcDNA-LINC01956 control cells. The expression levels of the M2 phenotype markers CD206 and MRC-2 were elevated in the pcDNA-LINC01956 group but not in the control group (Figure 6H). This finding indicates that exosomal LINC01956 promotes M2 polarization.

Collectively, our findings suggest that LINC01956 can be transferred via exosomes, thereby promoting M2 polarization of macrophages.

### **LINC01956 was transcriptionally regulated by HIF-1 $\alpha$ under hypoxic conditions**

Previous studies have demonstrated that a hypoxic TME might contribute to abnormal expression of some lncRNAs, including in GBM. We sought to determine whether LINC01956 is a hypoxia-sensitive lncRNA. We exposed GBM cells to hypoxia or normoxia for 48 h and revealed that HIF-1 $\alpha$  and LINC01956 expression levels were elevated (Figure 7A and B) under hypoxic conditions. The efficiency of HIF-1 $\alpha$  downregulation was examined by using western blotting (Figure 7C). Downregulation of HIF-1 $\alpha$  significantly inhibited LINC01956 expression under both normoxic and hypoxic conditions. In addition, downregulation of HIF-1 $\alpha$  counteracted hypoxia-induced LINC01956 upregulation (Figure 7D). We then explored whether HIF-1 $\alpha$  regulates LINC01956 by binding to its promoter. Via UCSC and JASPAR bioinformatics software, we analyzed the 1-kb region upstream of the transcription start site of LINC01956 and identified a putative HIF-1 $\alpha$  response element (HRE) in the LINC01956 promoter region (positions -367 to -372) (Figure 7E). To understand whether HIF-1 $\alpha$  regulates LINC01956 expression via this HRE, a vector carrying the wild-type LINC01956 promoter and a vector carrying the mutant LINC01956 promoter were constructed. There was an increase in luciferase activity in cells cotransfected with the pcDNA3-HIF-1 $\alpha$  plasmid and wild-type LINC01956 promoter. Luciferase activity was impaired in cells that were cotransfected with the pcDNA3-HIF-1 $\alpha$  plasmid and mutant LINC01956 promoter (Figure 7F).

Subsequently, the CHIP assay was carried out to confirm that HIF-1 $\alpha$  directly bound to the LINC01956 promoter (Figure 7G). Taken together, our findings imply that LINC01956 is regulated by HIF-1 $\alpha$ .

## Discussion

LncRNAs widely participate in regulating the initiation and progression of GBM and are useful diagnostic biomarkers and therapeutic targets for GBM[16, 17]. In our manuscript, we screened for abnormal expression of lncRNAs in GBM by using the TCGA database. We identified LINC01956 as a lncRNA that was upregulated in GBM samples. Interestingly, we also found that LINC01956 could be used as a prognostic factor in GBM patients. The biological function assays revealed that downregulation of LINC01956 suppressed cell growth and invasion. These data imply that LINC01956 may be an oncogene in GBM.

The mechanisms by which lncRNAs affect tumorigenesis are complicated[18]. Recently, it was reported that lncRNAs may exert their effects via specific interactions with functional proteins[19]. We thus explored whether LINC01956 exerted its effects by binding with specific proteins. Via the starBase database, we identified FUS, and by using a co-IP assay, we confirmed that LINC01956 directly interacted with FUS. Interestingly, our study elucidated the mechanism of LINC01956 forming a complex with FUS and  $\beta$ -catenin. This effect led to  $\beta$ -catenin nuclear translocation and thus activated Wnt/ $\beta$ -catenin signaling in glioma cells. Abnormal Wnt/ $\beta$ -catenin signaling plays an important role in pathologies, especially in human cancers[20]. Suppression of  $\beta$ -catenin inhibits multiple oncogenic targets in human glioma cells[21]. In the present study, we revealed that downregulation of LINC01956 decreased the activity of Wnt/ $\beta$ -catenin signaling in glioma cells. Our findings suggest that LINC01956 modulates the Wnt/ $\beta$ -catenin signaling pathway and promotes glioma progression.

Recently, studies have focused on the TME, a complex community that includes cancer cells, cancer-associated fibroblasts (CAFs), and immune/inflammatory cells[22]. TAMs, one of the most abundant immune cell populations in various solid cancers, are strongly associated with cancer cell proliferation and metastasis[23]. According to their different biological properties, macrophages can be classified into proinflammatory (M1) and anti-inflammatory (M2) macrophages[24]. TAMs, considered M2-like macrophages, are strongly correlated with cancer progression, including in glioma[25]. Our findings showed that LINC01956 was enriched in M2-like macrophages but not in M1-like macrophages or unpolarized macrophages. In addition, downregulation of LINC01956 significantly decreased the expression of M2-like macrophage markers. These data imply that LINC01956 is involved in M2 polarization. Interestingly, the supernatant from LINC01956-overexpressing cells contributed to increased expression of M2 markers, and this finding prompted us to explore the underlying mechanism mediating the communication between glioma cells and macrophages. Previous findings indicated that lncRNAs can be transferred via exosomes to regulate the TME[26]. In parallel, our findings revealed that glioma cell-derived exosomes promoted M2 polarization and thus exerted a tumor-promoting effect by transporting LINC01956.

As a universal phenomenon in a series of cancers, hypoxia is closely associated with cancer progression[27]. Previous studies have revealed that lncRNAs can be regulated by hypoxia via HIF-1 $\alpha$ -mediated transcriptional regulation[27]. A series of hypoxia-sensitive lncRNAs have been reported to be involved in tumorigenesis and tumor metastasis[28]. Similarly, we found that LINC01956 was regulated by HIF-1 $\alpha$  under hypoxic conditions. Hypoxia elevated the expression level of LINC01956, while this effect was abolished by downregulation of HIF-1 $\alpha$ . HIF-1 $\alpha$  usually regulates its downstream targets via HREs. Via the JASPAR database, we identified a potential

HRE in the promoter region of LINC01956. In addition, we identified the regulatory effect of HIF-1 $\alpha$  on LINC01956 transcription by CHIP and dual-luciferase reporter assays. Thus, our findings provide new evidence that supports the idea that LINC01956 acts as a link between hypoxia and glioma progression.

## Conclusion

Taken together, our data present the first evidence that LINC01956 is upregulated in GBM. LINC01956 plays an oncogenic role by forming a complex with FUS and  $\beta$ -catenin(Fig. 7H). Our data imply that the HIF-1 $\alpha$ /LINC01956/FUS/ $\beta$ -catenin axis is a potential therapeutic target for GBM.

## Abbreviations

Long noncoding RNAs

lncRNAs

glioblastoma

GBM

Tumor-associated macrophages

TAMs

polyvinylidene fluoride

PVDF

Chromatin immunoprecipitation

CHIP

RNA immunoprecipitation

RIP

Immunofluorescence

IF

Biolayer interferometry

BLI

Coimmunoprecipitation

co-IP

The Cancer Genome Atlas

TCGA

RNA-binding proteins

RBPs

## Declarations

### Funding

This work was supported by the Outstanding Youths Project of Shanxi Science and Technology Department(201901D211524).

### Author contributions

Xubin Deng designed and corresponded for the work. Gong Zhang, Fa Jin and Fengfei made the bioinformatic analysis and performed biological experiment. Lihong Zhao performed data analyses.

### **Ethics Approval and Consent to Participate**

This study was approved by the ethical review board of People's Hospital of Shanxi Province and Zhujiang Hospital, Southern Medical University. All of the patients were given and accepted informed consent form prior to their enrollment. All experimental procedures and animal care were reviewed and approved by the Animal Ethics Committee of People's Hospital of Shanxi Province and Zhujiang Hospital, Southern Medical University.

### **Conflicts of Interest**

The authors report no conflicts of interest in this work.

### **Consent for publication**

Not applicable.

### **Data Availability Statement**

All data are available upon request.

### **Specific statement**

This article has been published on a preprint server with its DOI: <https://doi.org/10.21203/rs.3.rs-358933/v1>.

## **References**

1. Reardon DA, Rich JN, Friedman HS, Bigner DD (2006) Recent advances in the treatment of malignant astrocytoma. *J Clin oncology: official J Am Soc Clin Oncol* 24(8):1253–1265. doi:10.1200/JCO.2005.04.5302
2. Iwamoto FM, Kreisl TN, Kim L, Duic JP, Butman JA, Albert PS, Fine HA (2010) Phase 2 trial of talampanel, a glutamate receptor inhibitor, for adults with recurrent malignant gliomas. *Cancer* 116(7):1776–1782. doi:10.1002/cncr.24957
3. Quinn JJ, Chang HY (2016) Unique features of long non-coding RNA biogenesis and function. *Nat Rev Genet* 17(1):47–62. doi:10.1038/nrg.2015.10
4. Prensner JR, Chinnaiyan AM (2011) The emergence of lncRNAs in cancer biology. *Cancer Discov* 1(5):391–407. doi:10.1158/2159-8290.CD-11-0209
5. Petty AJ, Yang Y (2017) Tumor-associated macrophages: implications in cancer immunotherapy. *Immunotherapy* 9(3):289–302. doi:10.2217/imt-2016-0135
6. Biswas SK, Gangi L, Paul S, Schioppa T, Sacconi A, Sironi M, Bottazzi B, Doni A, Vincenzo B, Pasqualini F, Vago L, Nebuloni M, Mantovani A, Sica A (2006) A distinct and unique transcriptional program expressed by tumor-associated macrophages (defective NF-kappaB and enhanced IRF-3/STAT1 activation). *Blood* 107(5):2112–2122. doi:10.1182/blood-2005-01-0428

7. Huang JK, Ma L, Song WH, Lu BY, Huang YB, Dong HM, Ma XK, Zhu ZZ, Zhou R (2017) LncRNA-MALAT1 Promotes Angiogenesis of Thyroid Cancer by Modulating Tumor-Associated Macrophage FGF2 Protein Secretion. *J Cell Biochem* 118(12):4821–4830. doi:10.1002/jcb.26153
8. Han D, Fang Y, Guo Y, Hong W, Tu J, Wei W (2019) The emerging role of long non-coding RNAs in tumor-associated macrophages. *J Cancer* 10(26):6738–6746. doi:10.7150/jca.35770
9. Ma L, Zhang G, Miao XB, Deng XB, Wu Y, Liu Y, Jin ZR, Li XQ, Liu QZ, Sun DX, Testa JR, Yao KT, Xiao GH (2013) Cancer stem-like cell properties are regulated by EGFR/AKT/beta-catenin signaling and preferentially inhibited by gefitinib in nasopharyngeal carcinoma. *FEBS J* 280(9):2027–2041. doi:10.1111/febs.12226
10. Li XQ, Yang XL, Zhang G, Wu SP, Deng XB, Xiao SJ, Liu QZ, Yao KT, Xiao GH (2013) Nuclear beta-catenin accumulation is associated with increased expression of Nanog protein and predicts poor prognosis of non-small cell lung cancer. *J Transl Med* 11:114. doi:10.1186/1479-5876-11-114
11. Tian X, Wu Y, Yang Y, Wang J, Niu M, Gao S, Qin T, Bao D (2020) Long noncoding RNA LINC00662 promotes M2 macrophage polarization and hepatocellular carcinoma progression via activating Wnt/beta-catenin signaling. *Mol Oncol* 14(2):462–483. doi:10.1002/1878-0261.12606
12. Liang Y, Song X, Li Y, Chen B, Zhao W, Wang L, Zhang H, Liu Y, Han D, Zhang N, Ma T, Wang Y, Ye F, Luo D, Li X, Yang Q (2020) LncRNA BCRT1 promotes breast cancer progression by targeting miR-1303/PTBP3 axis. *Mol Cancer* 19(1):85. doi:10.1186/s12943-020-01206-5
13. Ni W, Yao S, Zhou Y, Liu Y, Huang P, Zhou A, Liu J, Che L, Li J (2019) Long noncoding RNA GAS5 inhibits progression of colorectal cancer by interacting with and triggering YAP phosphorylation and degradation and is negatively regulated by the m(6)A reader YTHDF3. *Mol Cancer* 18(1):143. doi:10.1186/s12943-019-1079-y
14. Garcia C, Dubois LG, Xavier AL, Geraldo LH, da Fonseca AC, Correia AH, Meirelles F, Ventura G, Romao L, Canedo NH, de Souza JM, de Menezes JR, Moura-Neto V, Tovar-Moll F, Lima FR (2014) The orthotopic xenotransplant of human glioblastoma successfully recapitulates glioblastoma-microenvironment interactions in a non-immunosuppressed mouse model. *BMC Cancer* 14:923. doi:10.1186/1471-2407-14-923
15. Xue M, Chen W, Xiang A, Wang R, Chen H, Pan J, Pang H, An H, Wang X, Hou H, Li X (2017) Hypoxic exosomes facilitate bladder tumor growth and development through transferring long non-coding RNA-UCA1. *Mol Cancer* 16(1):143. doi:10.1186/s12943-017-0714-8
16. Liu X, Zhu Q, Guo Y, Xiao Z, Hu L, Xu Q (2019) LncRNA LINC00689 promotes the growth, metastasis and glycolysis of glioma cells by targeting miR-338-3p/PKM2 axis. *Biomed pharmacotherapy = Biomedecine pharmacotherapie* 117:109069. doi:10.1016/j.biopha.2019.109069
17. Yao X, Li X, Luo Y, Xu X, Liu J, Bu J (2020) LncRNA GAS5 Regulates Osteosarcoma Cell Proliferation, Migration, and Invasion by Regulating RHOB via Sponging miR-663a. *Cancer Manag Res* 12:8253–8261. doi:10.2147/CMAR.S251881
18. (!!! INVALID CITATION !!! [18; 19])
19. Wang Y, Lu JH, Wu QN, Jin Y, Wang DS, Chen YX, Liu J, Luo XJ, Meng Q, Pu HY, Wang YN, Hu PS, Liu ZX, Zeng ZL, Zhao Q, Deng R, Zhu XF, Ju HQ, Xu RH (2019) LncRNA LINRIS stabilizes IGF2BP2 and promotes the aerobic glycolysis in colorectal cancer. *Mol Cancer* 18(1):174. doi:10.1186/s12943-019-1105-0
20. Bordonaro M, Tewari S, Cicco CE, Atamna W, Lazarova DL (2011) A switch from canonical to noncanonical Wnt signaling mediates drug resistance in colon cancer cells. *PLoS ONE* 6(11):e27308.

doi:10.1371/journal.pone.0027308

21. He L, Zhou H, Zeng Z, Yao H, Jiang W, Qu H (2019) Wnt/beta-catenin signaling cascade: A promising target for glioma therapy. *J Cell Physiol* 234(3):2217–2228. doi:10.1002/jcp.27186
22. Hinshaw DC, Shevde LA (2019) The Tumor Microenvironment Innately Modulates Cancer Progression. *Cancer Res* 79(18):4557–4566. doi:10.1158/0008-5472.CAN-18-3962
23. Dymicka-Piekarska V, Koper-Lenkiewicz OM, Zinczuk J, Kratz E, Kaminska J (2021) Inflammatory cell-associated tumors. Not only macrophages (TAMs), fibroblasts (TAFs) and neutrophils (TANs) can infiltrate the tumor microenvironment. The unique role of tumor associated platelets (TAPs). *Cancer immunology, immunotherapy: CII* 70. 1497–1510. doi:10.1007/s00262-020-02758-7. 6
24. Kim J, Bae JS (2016) Tumor-Associated Macrophages and Neutrophils in Tumor Microenvironment. *Mediat Inflamm* 2016:6058147. doi:10.1155/2016/6058147
25. Komohara Y, Fujiwara Y, Ohnishi K, Takeya M (2016) Tumor-associated macrophages: Potential therapeutic targets for anti-cancer therapy. *Adv drug delivery reviews* 99 (Pt B) 180–185. doi:10.1016/j.addr.2015.11.009
26. Xiao M, Zhang J, Chen W, Chen W (2018) M1-like tumor-associated macrophages activated by exosome-transferred THBS1 promote malignant migration in oral squamous cell carcinoma. *J experimental Clin cancer research: CR* 37(1):143. doi:10.1186/s13046-018-0815-2
27. Henze AT, Mazzone M (2016) The impact of hypoxia on tumor-associated macrophages. *J Clin Investig* 126(10):3672–3679. doi:10.1172/JCI84427
28. Hua Q, Mi B, Xu F, Wen J, Zhao L, Liu J, Huang G (2020) Hypoxia-induced lncRNA-AC020978 promotes proliferation and glycolytic metabolism of non-small cell lung cancer by regulating PKM2/HIF-1alpha axis. *Theranostics* 10(11):4762–4778. doi:10.7150/thno.43839

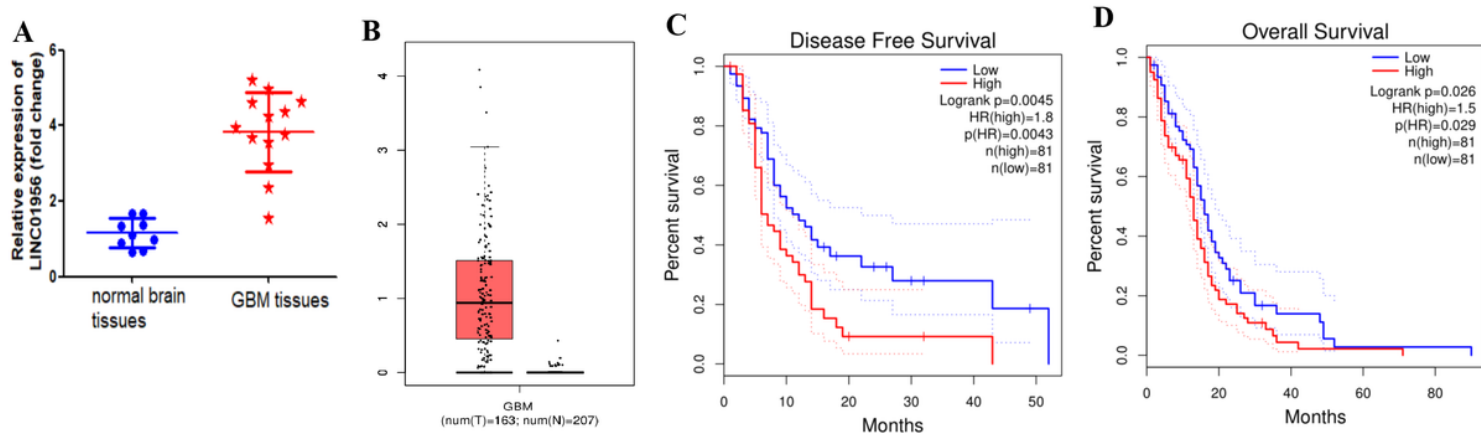
## Tables

Table 1

Univariate and multivariate analysis of clinicopathological factors that correlate with OS of glioma patients

| Characteristics                                | Total(N) | Univariate analysis     |         | Multivariate analysis  |         |
|--|----------|-------------------------|---------|------------------------|---------|
|  |          | Hazard ratio (95% CI)   | P value | Hazard ratio (95% CI)  | P value |
| WHO grade                                      | 634      |                         |         |                        |         |
| G2   | 223      |                         |         |                        |         |
| G3&G4  | 411      | 5.642<br>(3.926–8.109)  | < 0.001 | 1.842<br>(1.203–2.822) | 0.005   |
| 1p/19q codeletion                              | 688      |                         |         |                        |         |
| codel  | 170      |                         |         |                        |         |
| non-codel                                      | 518      | 4.428<br>(2.885–6.799)  | < 0.001 | 1.796<br>(1.075–3.000) | 0.025   |
| IDH status                                     | 685      |                         |         |                        |         |
| WT   | 246      |                         |         |                        |         |
| Mut  | 439      | 0.117<br>(0.090–0.152)  | < 0.001 | 0.320<br>(0.219–0.468) | < 0.001 |
| LINC01956                                      | 695      |                         |         |                        |         |
| Low  | 348      |                         |         |                        |         |
| High   | 347      | 3.648<br>(2.805–4.745)  | < 0.001 | 2.120<br>(1.559–2.883) | < 0.001 |
| Histological type                              | 695      |                         |         |                        |         |
| Astrocytoma&Oligoastrocytoma&Oligodendroglioma | 527      |                         |         |                        |         |
| Glioblastoma                                   | 168      | 9.114<br>(7.008–11.853) | < 0.001 | 2.733<br>(1.961–3.808) | < 0.001 |

## Figures



**Figure 1**

The expression level of LINC01956 was elevated in GBM tissues and associated with poor clinical outcome.

(A) RT-PCR assay was used to examine LINC01956 expression levels in GBM tissues and normal brain tissues. (B) LINC01956 expression level was indicated in GBM tissues and normal brain tissues, data from TCGA database. (C) GBM patients with high expression level of LINC01956 tend to have poorer disease-free survival rate than those with low expression level of LINC01956. (D) GBM patients with high expression level of LINC01956 tend to have poorer overall survival rate than those with low expression level of LINC01956.

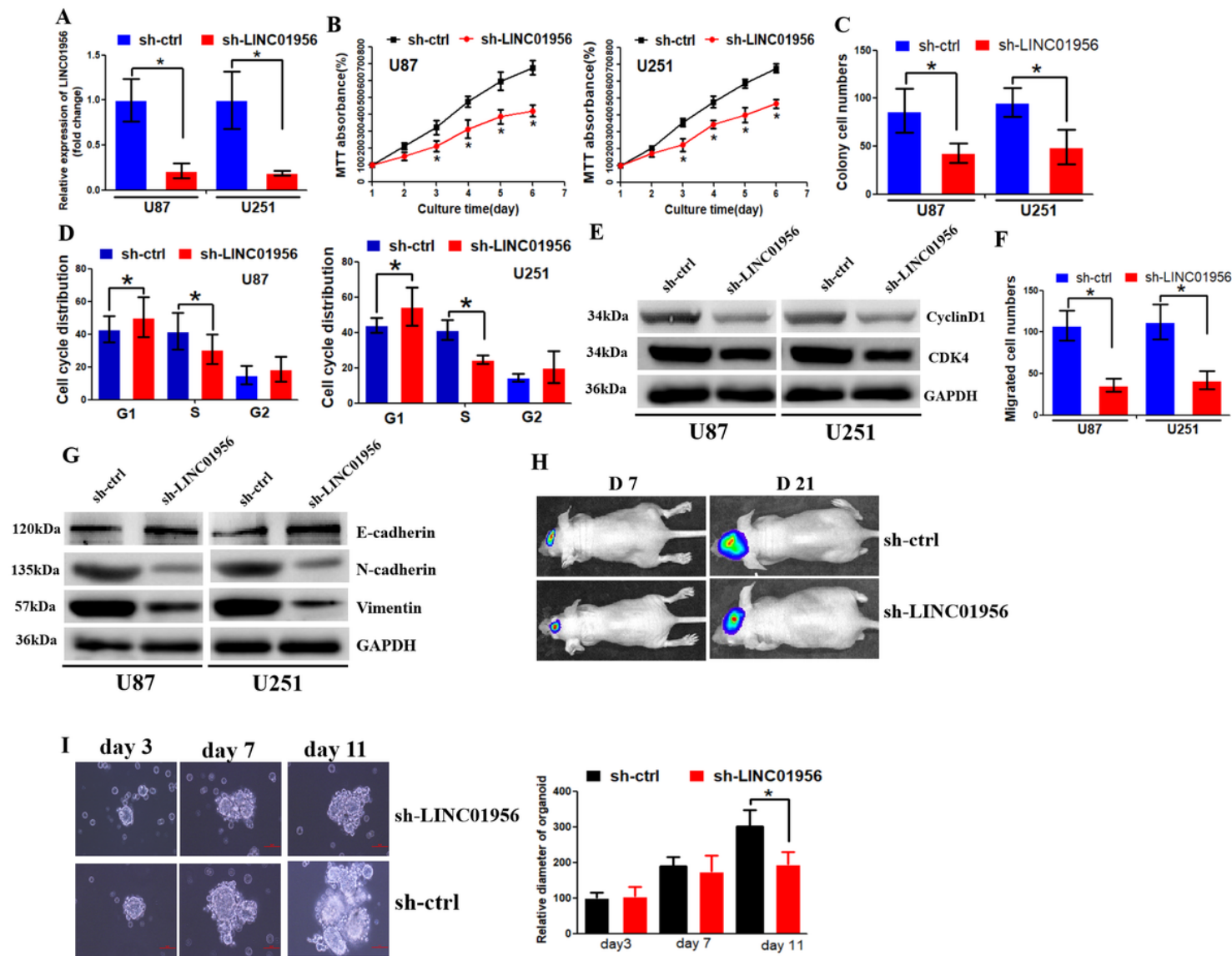


**Figure 2**

**LINC01956 inhibition decreased GBM cell growth and invasion.**

(A) RT-PCR assay was used to examine LINC01956 expression levels in sh-ctrl and sh-LINC01956 cells, respectively. (B) MTT assay was used to examine cell viability. (C) The colony formation assay was used to measure cell colony formation ability. (D) The flow cytometry assay was used to examine cell cycle distribution. (E) Western blot assay was used to examine protein expression levels. (F) Boyden assay was used to test cell invasion ability. (G) Western blot assay was used to examine expression levels of E-cadherin, N-cadherin and Vimentin. (H) An orthotopic glioma xenograft model was established to monitor LINC01956's effect on cell growth in vivo. (I) Representative images (scale bar: 100  $\mu$ m) and quantification of organoid size.

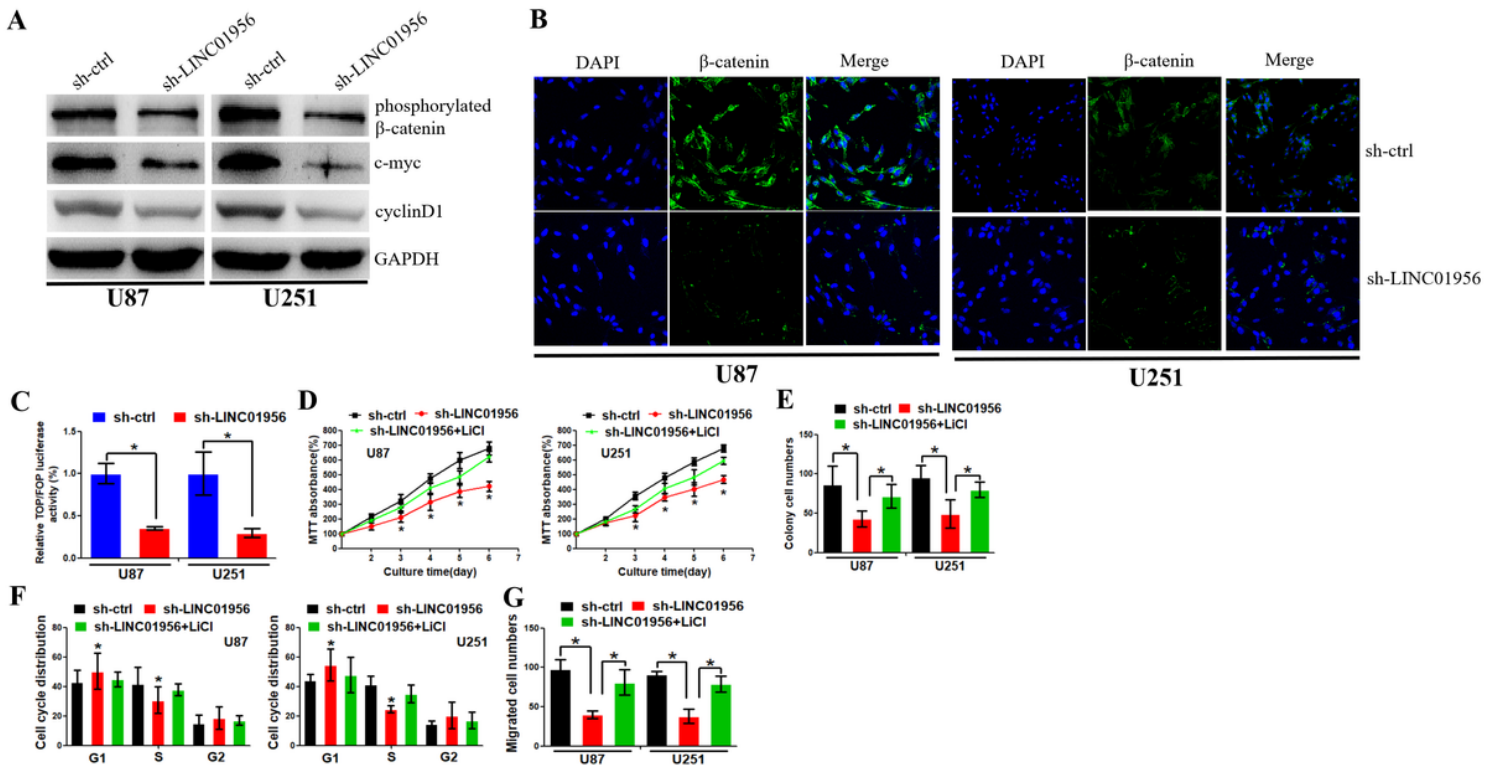


**Figure 3**

**LINC01956 promoted GBM cell progression via WNT/ $\beta$ -catenin signaling pathway.**

(A) Western blot assay was used to examine protein expression levels. (B) The immunofluorescence assay was used to examine  $\beta$ -catenin cellular position. (C) TOP/FOP flash reporter assay was performed to examine  $\beta$ -catenin activity. (D) MTT assay was used to examine cell viability. (E) Colony formation assay was used to measure cell proliferative ability. (F) The flow cytometry assay was used to examine cell cycle distribution. (G) Boyden assay was used to test cell invasion ability.

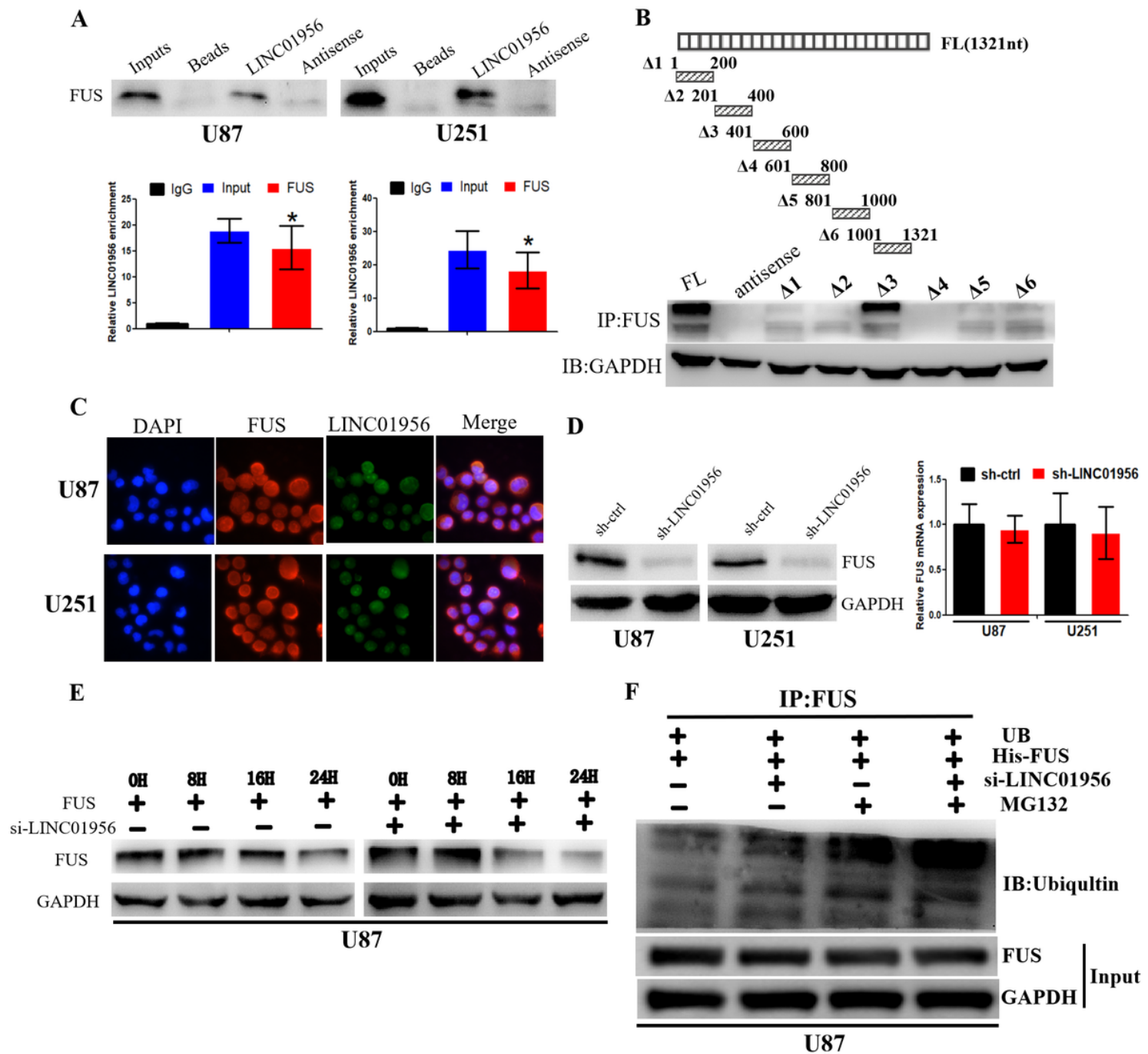


**Figure 4**

**LINC01956 bound to FUS and reduced its ubiquitination.**

(A) The RNA pull-down and RIP assays were performed to examine interaction between LINC01956 and FUS. (B) Bio-layer interferometry (BLI) analysis of biotinylated-LINC01956 binding to FUS protein. (C) The immunofluorescence assay was used to examine cellular location of LINC01956 and FUS. (D) Down-regulation of LINC01956 decreased FUS protein expression level (left panel). Down-regulation of LINC01956 did not affect FUS mRNA expression level (right panel). (E) Cycloheximide (CHX) chase assay combined with western blot assay were used to examine FUS protein stability. (F) Western blot assay was used to analyze ubiquitination of FUS protein.

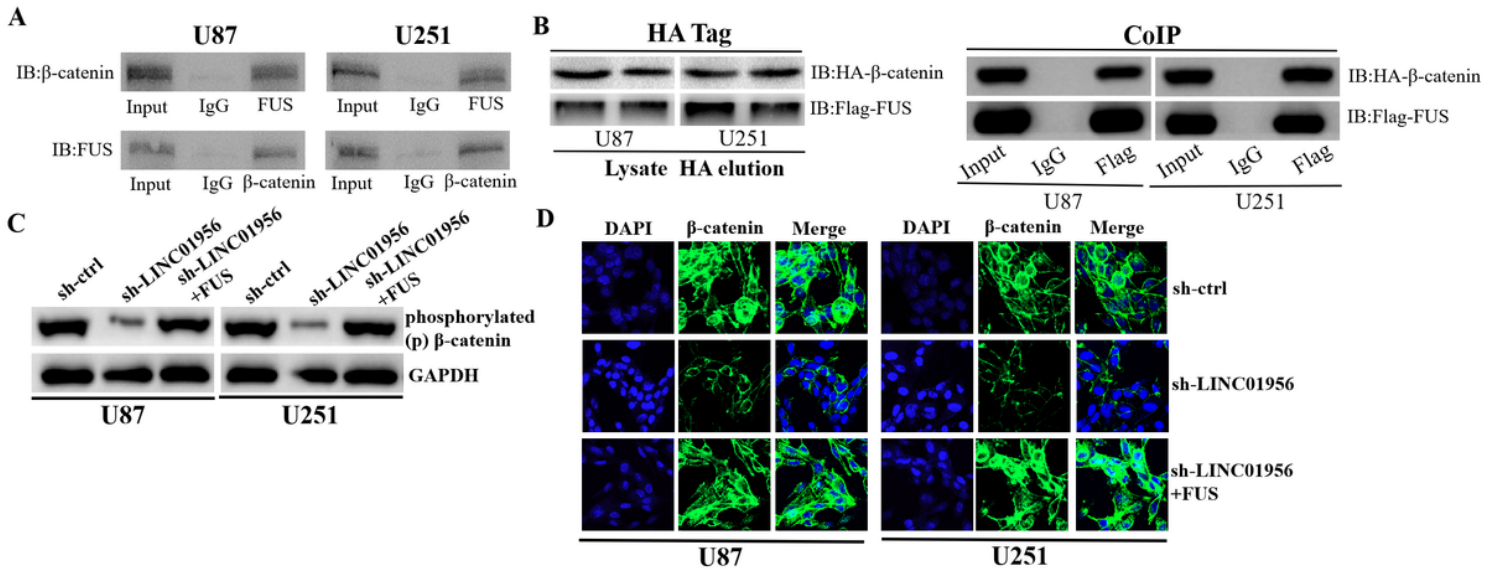


Figure 5

LINC01956 facilitates the translocation of  $\beta$ -catenin into the nucleus of GBM cells through recruiting FUS

(A) The interaction between FUS and  $\beta$ -catenin was proved by co-IP assay. (B) The existence of the complex containing LINC01956, FUS, and  $\beta$ -catenin was validated using two-step coIP assay. (C) Western blot assay was used to examine protein expression levels. (D) The immunofluorescence assay indicated that down-regulation of LINC01956 inhibited nuclear translocation of  $\beta$ -catenin, which was abrogated in the context of FUS con-transfection.

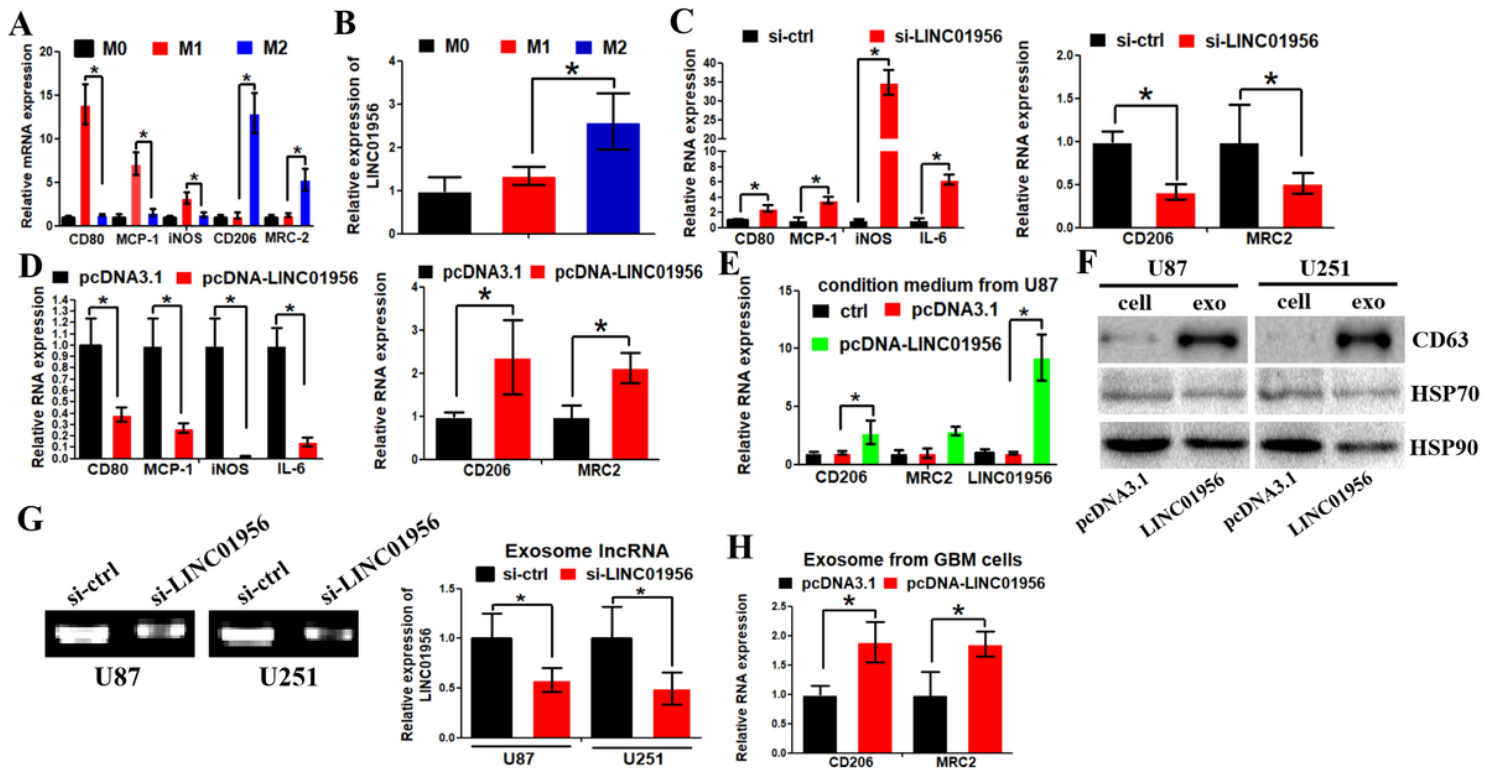


Figure 6

## Exosomal LINC01956 promoted M2 phenotype polarization in GBM cells

(A) M1 macrophages-associated genes and M2 macrophages-associated genes were examined by RT-PCR assay. (B) LINC01956 expression level was examined in M1 and macrophages, respectively. (C) Down-regulation of LINC01956 decreased M2 macrophages markers. (D) Over-expression of LINC01956 increased M2 macrophages markers. (E) Conditioned medium derived from LINC01956-overexpressing cells increased the expression of M2 markers and LINC01956 in macrophages. (F) The western blot assay was used to examine exosome-related proteins. (G) Agarose gel electrophoresis and RT-PCR assays were used to detect the expression of LINC01956 in exosomes. (H) The expression of M2 markers and LINC01956 in macrophages was examined after culture with the indicated exosomes.

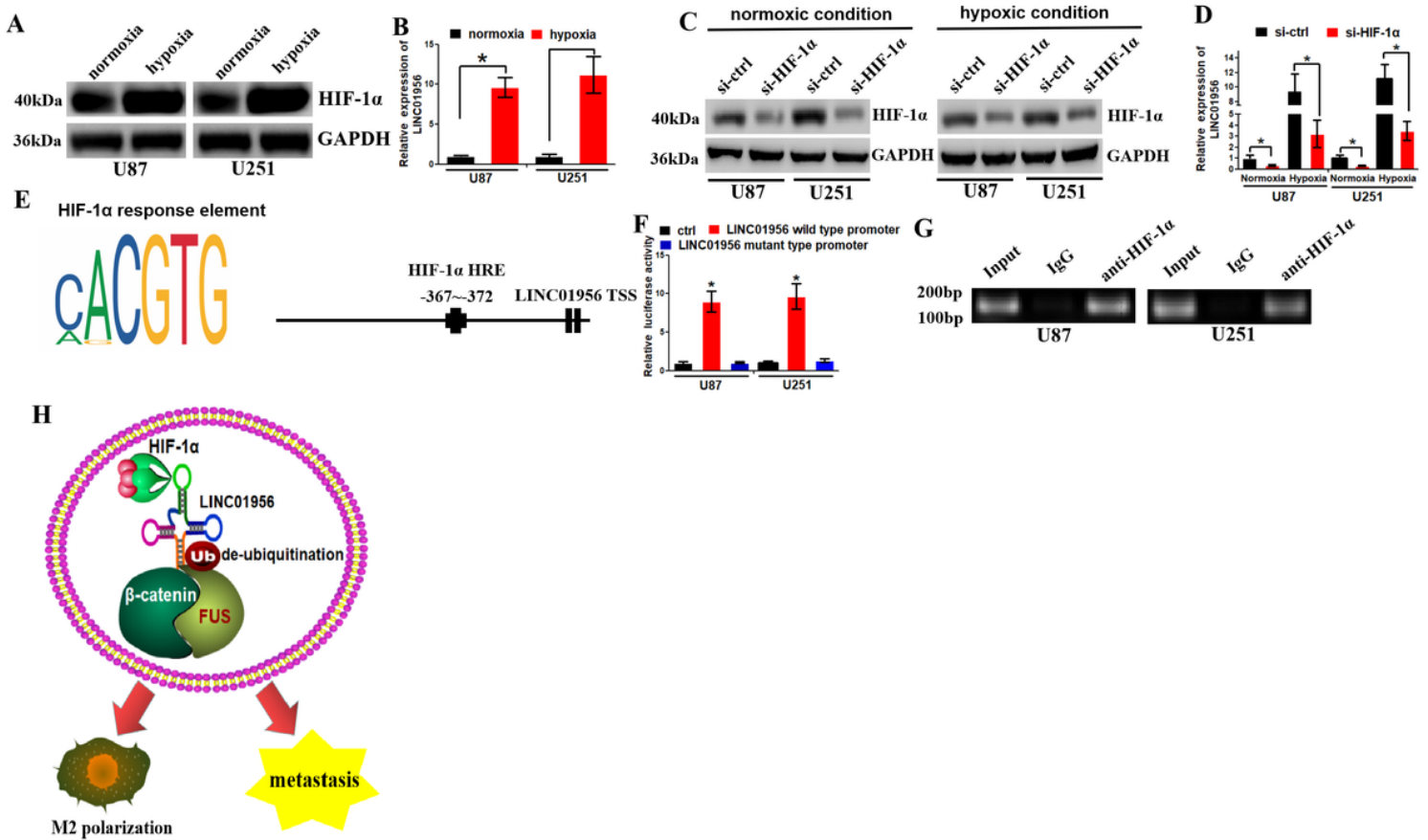


Figure 7

### LINC01956 was transcriptionally regulated by HIF-1α under hypoxic conditions

(A) and (B) The expression levels of HIF-1α protein or LINC01956 were examined by western blot or RT-PCR assays after culture under normoxia or hypoxia. (C) The efficiency of HIF-1α down-regulation was examined by using western blot. (D) HIF-1α down-regulation decreased the expression of LINC01956 under normoxia or hypoxia condition. (E) The recognition motif of HIF-1α was obtained from the JASPAR database. (F) Luciferase activity was examined with the dual-luciferase reporter assay system. (G) PCR gel showing amplification of HIF-1α-binding site after ChIP using antibody against HIF-1α. (H) Working model of LINC01956 regulated by HIF-1α in activating β-catenin via the de-ubiquitination of FUS in glioma.

## Supplementary Files

This is a list of supplementary files associated with this preprint. Click to download.

- [supplementarydata.docx](#)